Proceedings 10th NUMGE 2023
10th European Conference on Numerical Methods in Geotechnical Engineering
Zdravkovic L, Kontoe S, Taborda DMG, Tsiampousi A (eds)

https://doi.org/10.53243/NUMGE2023-125

Cone penetration in brittle, lightly over-consolidated soils: a numerical perspective

L. Monforte[1], M. Arroyo[1,2], A. Gens[1,2]

[1]*Centre Internacional de Mètodes Numèrics Enginyeria (CIMNE), Barcelona, SPAIN*
[2]*Universitat Politècnica de Catalunya (UPC-BarcelonaTECH), Barcelona, SPAIN*

ABSTRACT: In this paper, cone penetration testing is simulated in potentially liquefiable soils using the Geotechnical Particle Finite Element method, specially designed for the analysis of penetration problems in geomechanics. The material response is modelled with CASM, a critical state, state-parameter dependent model. The paper reports a parametric analysis of cone testing in undrained liquefiable geomaterials, that covers the effect of brittleness and over-consolidation ratio of the geomaterial as well as the friction angle at the soil-cone interface.

Keywords: static liquefaction, CPTu, overconsolidation, CASM, large strain

1 INTRODUCTION

Static liquefaction is characterized by a sudden drop of the undrained shear strength in undrained conditions. The constitutive response of potentially liquefiable geomaterials might be explained in the context of critical state soil mechanics. A soil will have a dilatant behaviour if the void ratio is smaller than the void ratio at the critical state line at the same stress level; in contrast, if the void ratio is larger than that at critical state conditions at the same mean effective stress, the material will have a contractive behaviour and might be prone to static liquefaction. Therefore, the state parameter -defined as the difference between the current void ratio and that at the critical state line at the same mean effective stress- can be used to characterize the material response; positive values correspond to a contractive response and negative to a dilative response.

Geomaterials that may potentially liquefy give little warning of the impending failure and the consequences of failure are generally momentous. For example, static liquefaction was involved in the failure of the mine tailing storage facilities of Merriespruit (Fourie et al., 2001) and Brumadinho (Arroyo and Gens, 2021). The thorough characterization of geomaterials that can liquefy is therefore crucial.

These geomaterials are typically characterized by means of in situ tests, predominantly by the cone penetration test (CPTu). Several techniques to infer the state parameter from CPTu readings have been proposed, based on empiricism (Plewes et al., 1992), cavity expansion (Jefferies and Been, 2016), numerical modelling (Pezeshki and Ahmadi, 2022) or a combination of numerical modelling and cavity expansion (Monforte et al., 2023a). When applied to interpret a CPTu record, these techniques show a good qualitative agreement (i.e. all interpretation methods will coincide in predicting that the soil will exhibit contractive behaviour) but not quantitatively, as the range of inferred state parameters is large (Monforte et al., 2023b).

Recently, the authors reported a parametric analysis of CPTu in undrained, almost normally consolidated soils (Monforte et al., 2023a). The analysis explored the effect of soil constitutive parameters in the relation between the initial state parameter and cone metrics in undrained conditions. It turned out that the numerical results could be summarized by an analytical cavity expansion expression provided that correction terms to tackle the geometrical mismatch between cone testing and cavity expansion are included.

The analysis referred to above focused on normally consolidated materials. This is a condition representative for many geomaterials susceptible to flow liquefaction, but not all. For instance, moist tamped sands with OCR as high as 4 have been shown to liquefy under static loading (Mahmoudi et al., 2020). It was then interesting to extend the previous numerical analysis to examine the effect of moderate overconsolidation.

2 SIMULATION PROGRAM

Numerical simulations of CPTu testing are performed using GPFEM (Monforte et al., 2018; Carbonell et al., 2022), which has been developed for the analysis of large-strain problems in geomechanics, including the contact with rigid and deformable structures. PFEM (Oñate et al., 2004) is based on a Lagrangian description of the motion, the use of low order finite elements to

compute the solution and the constant regeneration of the finite element mesh describing the domain.

Cone penetration is simulated employing an axisymmetric model. The cone is whished-in-place at a depth of 10 radii and it is pushed at the standard velocity of 0.02 m/s. Null displacements are prescribed at the bottom domain, whereas null radial displacements are prescribed on the vertical boundaries. Drainage is only allowed at the bottom of the domain. The initial effective vertical stress is equal to 100 kPa and K_0 is computed with Jaky's formula.

A coupled hydromechanical formulation is employed and the soil is discretized with linear triangular elements. In order to alleviate the severe volumetric locking that these elements suffer from the quasi-incompressible response due to undrained conditions and to the effective constitutive response at critical state, a mixed stabilized formulation is adopted where the degrees of freedom are displacements, Jacobian (volume change) and pore water pressure (Monforte et al., 2017).

The effective constitutive response of the soil is described by the isotropic, critical state-based model CASM (clay and sand model) (Yu, 1998). In the compression plane, both the isotropic compression line (ICL) and critical state line (CSL) are straight and parallel, expressed, respectively, as:

$$e(p') = e_0 - \lambda \ln p' \qquad (1)$$

$$\Gamma(p') = e_0 - (\lambda - \kappa) \ln r - \lambda \ln p' \qquad (2)$$

where p' is mean effective stress, λ and κ are the slope of the virgin loading and reloading curves at the $\ln p' - e$ plane, e_0 is the void ratio at 1 kPa and r is the spacing ratio, a constitutive parameter controlling the vertical distance between the ICL and CSL.

The mathematical expression for the yield surface is given by:

$$f = \left(\frac{q}{Mp'}\right)^n + \frac{1}{\ln r} \ln\left(\frac{p'}{p_c}\right) \qquad (3)$$

where q is the deviatoric stress, p_c the preconsolidation stress, M is the slope of the CSL in the $p' - q$ plane and n is a constitutive parameter controlling the shape of the yield surface.

The constitutive model is completed by an elastic model in which the bulk and shear modulus depend on the mean effective stress and the flow rule proposed by Mánica et al. (2021).

In the present work five different sets of constitutive parameters are employed, that differ in the distance between the ICL and CSL. All the materials share the same ICL but the CSLs are different. Table 1 and 2 list the constitutive parameters as well as the initial state parameter and the peak and residual undrained shear strength.

To illustrate the material response of the materials with the highest and lowest residual undrained shear strength, Figure 1 shows the simulation of undrained triaxial tests for values of overconsolidation ratio (OCR) of 1.6 and 1.1. The initial stress state of these element tests is the same than the one that will be used in the simulations of CPTu testing: $\sigma'_v = 100$ kPa and $\sigma'_h = 60.1$ kPa for OCR = 1.1 and $\sigma'_h = 70.4$ kPa for OCR = 1.6.

All materials have a contractive behavior, and even material E, with an OCR of 1.6 and an initial state parameter of $\psi_0 = 0.01$ exhibits brittle behavior.

Table 1. Adopted constitutive parameters and initial state parameter. The parameters, $\kappa = 0.016$, $\lambda = 0.053$, $\phi = 25º$, $e_{100} = 1.0$ and $\nu = 0.3$ are the same for all materials.

Material	n	r	ψ_0 OCR = 1.1	ψ_0 OCR = 1.6
A	10	12	0.089	0.078
B	10	8	0.074	0.063
C	9	6	0.063	0.052
D	7	3	0.036	0.026
E	4	2	0.020	0.010

Table 2. Peak and residual undrained shear strength.

Material	S_u^{peak} (kPa) OCR = 1.1	S_u^{res} (kPa) OCR = 1.1	S_u^{peak} (kPa) OCR = 1.6	S_u^{res} (kPa) OCR = 1.6
A	26.12	6.77	32.58	9.04
B	26.54	8.98	32.22	11.98
C	26.31	11.02	32.18	14.70
D	26.46	18.03	33.99	24.06
E	26.70	24.92	35.38	33.26

3 NUMERICAL RESULTS

Figure 2 shows the results of the CPTu simulation assuming a smooth soil-cone interface using an OCR = 1.6. For comparison purposes, results with an OCR equal to 1.1 are also included (Monforte et al., 2023a). Net cone resistance is defined as $q_n = q_c - \sigma_{v0}$, where q_c is the cone resistance and σ_{v0} the initial total vertical stress. In all the simulations, steady state conditions in the net cone resistance and the excess pore pressure at the u_2 position are achieved after a penetration of 10 cone radii. Both, the net cone resistance and the excess pore pressure when the initial state parameter reduces. For every material, increasing the OCR increases the net cone resistance and the excess pore pressure; the effect is much more pronounced in material E, with the lowest sensitivity.

Steady state normalized cone metrics from the numerical simulations are reported in Figure 3 in terms of the initial state parameter of the soil. The normalized

cone resistance, $Q_p = \frac{(q_c - p_0)}{p_0'}$, and the normalized effective cone resistance, $Q_p(1 - B_q) + 1 = \frac{(q_c - u_2)}{p_0'}$, increase by decreasing the state parameter, whereas the excess pore pressure ratio, $B_q = \frac{\Delta u_2}{q_c - p_0}$, decreases with the state parameter for both cone face and cone shoulder measurements.

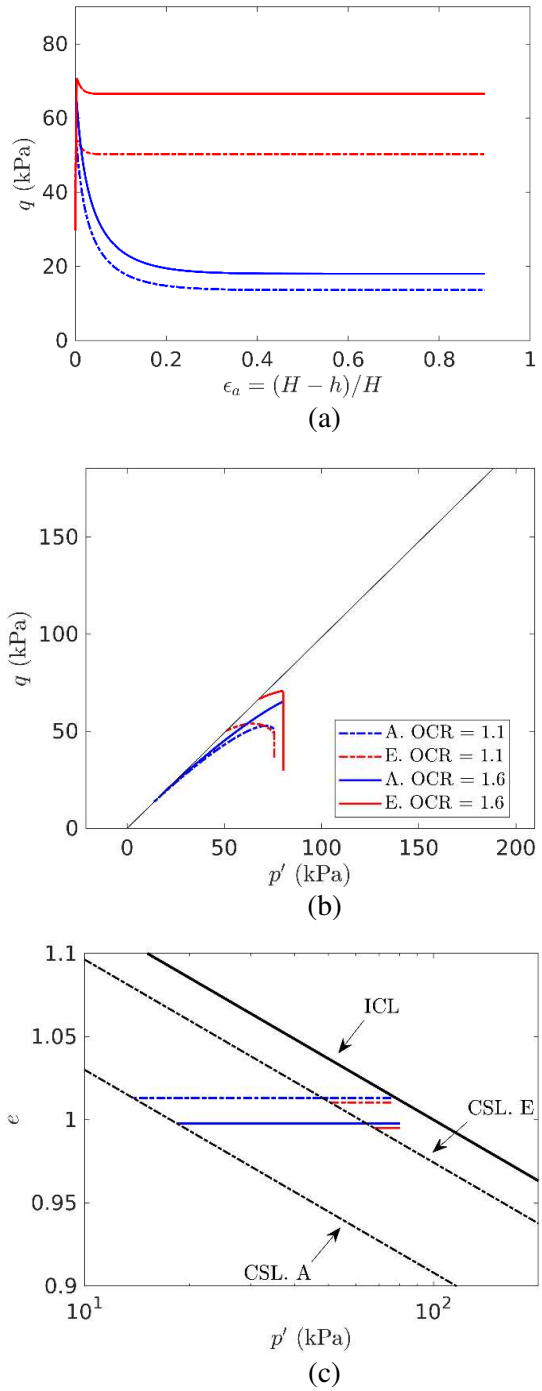

Figure 1. Simulation of undrained triaxial loading for materials A and E with different over-consolidation ratios.

For completeness, Figure 3 also reports the solution of the infinite expansion of a cylindrical and spherical cavity in undrained, CASM material (Mo and Yu, 2017). Qualitatively, Q_p and B_q follow the same trends; of course, there is not a quantitative agreement as the geometry of both problems -cone testing and cavity expansion- are different. The normalized effective tip resistance computed using the midface reading, u_1 position, shows a remarkable agreement with the solution of cavity expansion theory.

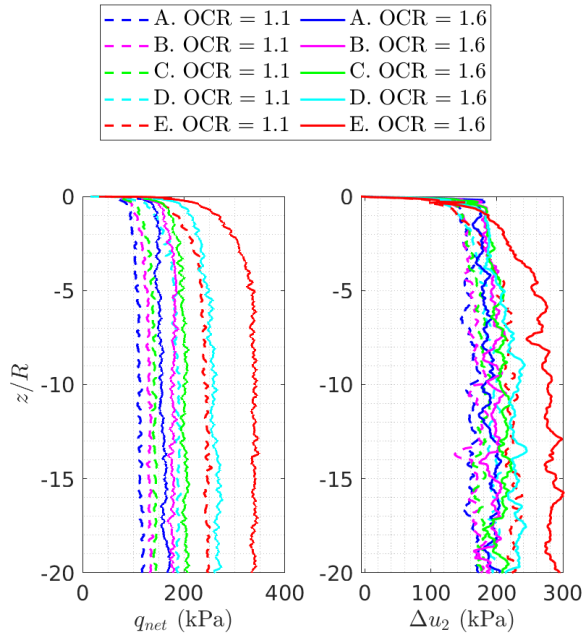

Figure 2. Net cone resistance and excess pore pressure at the u_2 position against normalized penetration.

This result is not fortuitous but a consequence of the stress state at the tip of the cone. In that location, the soil is at critical state and the largest principal effective stress is normal to the tip of the cone (since the interface is considered smooth), see Figure 4(b); the other two principal stresses are equal; thus, the soil is in triaxial compression conditions. The excess pore pressure is quite uniform at the tip of the cone, see Figure 5(b). Prescribing force equilibrium at the tip of the cone and assuming that (i) the excess pore pressure at the tip of the cone is uniform and equal to u_1 and (ii) the effective stress state of the soil is at critical state conditions and the major principal effective stress is normal to the cone tip, the normalized effective cone resistance can be expressed as (Monforte et al., 2023a):

$$Q_p\left(1 - B_{q1}\right) + 1 = \frac{q_c - u_1}{p_0'} = \qquad (4)$$

$$= \left(1 + \frac{2M}{3}\right)\exp\left(-\frac{\psi}{\lambda}\right)$$

which also corresponds to the normalized effective resistance of a spherical cavity.

To extend the scope of the analyses, the same simulations have been re-run considering this time a rough interface: a 18° interface friction angle has been used for

the soil-steel interface. As expected, the net cone resistance increases when the interface friction angle is not zero (Figure 3). The opposite effect is observed in the pore pressure ratio. However, the excess pore pressure is mostly unaffected by the interface behaviour (Figure 5).

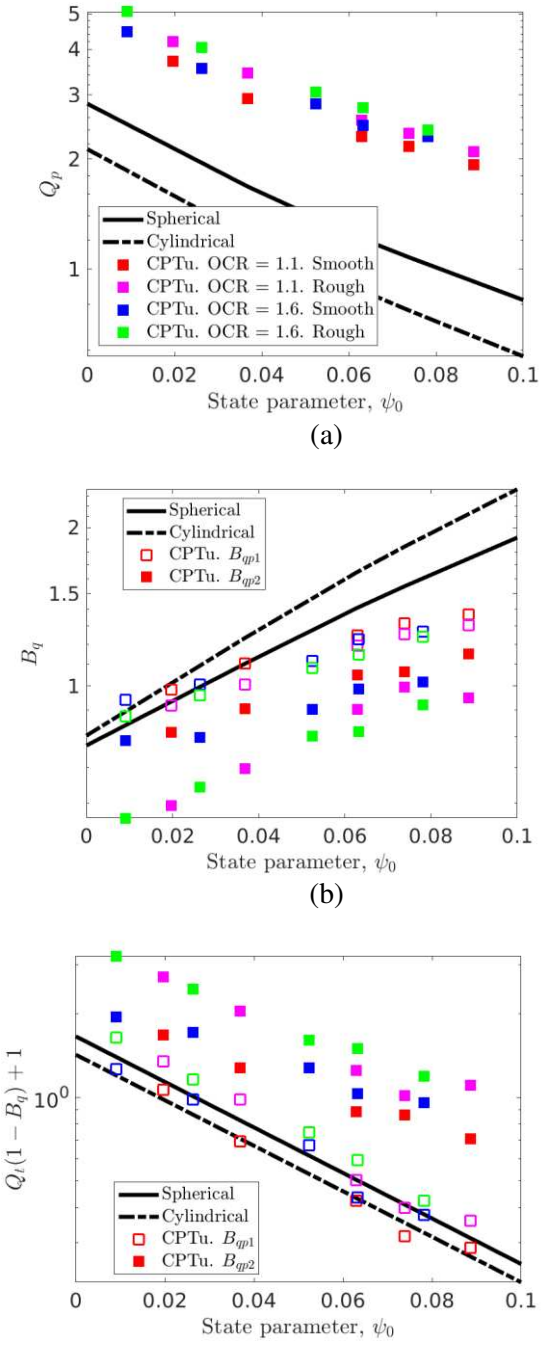

Figure 3. Variation of normalized cone resistance (a), excess pore pressure ratio(b) and normalized effective tip resistance (c) with initial state parameter.

The larger normalized effective cone resistance when considering a rough interface can also be explained by the stress state of the soil just beneath the tip of the cone. Again, the soil is at critical state in triaxial compression conditions. This time, however, the major principal stress direction is not normal to the cone tip as in the smooth case but is more vertical (see Figure 4).

Equation (4), based on the equilibrium of forces, can be further modified to reflect that the soil-steel interface is not smooth. Again, based on the constitutive response of the soil and equilibrium at the cone tip, the normalized effective tip resistance may be expressed as (Monforte et al., 2023a):

$$Q_p\left(1-B_{q1}\right)+1=c_q\left(1+\frac{2M}{3}\right)\exp\left(-\frac{\psi}{\lambda}\right) \quad (5)$$

where c_q is a geometric term taking into acount the roughness of the cone, the range of which is in the rnage $c_q \in \left[1, \frac{7M+6}{4M+6}\right]$.

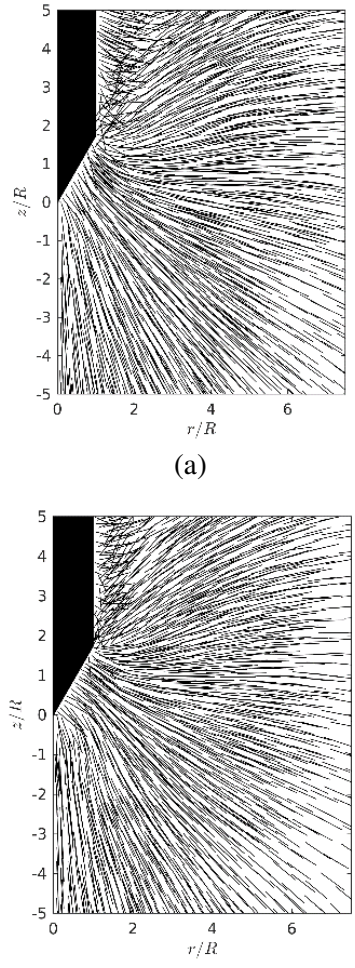

Figure 4. Comparison of the major principal effective stress for a rough soil-cone interface (a) and smooth interface (b). Material E. OCR = 1.6.

4 INTERPRETATION METHOD

In undrained conditions, the state parameter is generally inferred from the normalized effective tip resistance, $Q_p\left(1-B_q\right)+1=(q_c-u_2)/p_0'$. The numerical results obtained in this work show a remarkable agreement with the cavity expansion solution but only if the rarely measured excess pore pressure at the u_1 position

is used. It is proposed therefore to modify Equation (5) by taking into account that the excess pore pressures at the two locations are related through $\Delta u_1 = \beta\, \Delta u_2$. So:

$$Q_p \left(1 - \beta B_{q2}\right) + 1 = c_q \left(1 + \frac{2M}{3}\right) \exp\left(-\frac{\psi}{\lambda}\right) \quad (6)$$

Figure 6 reports Equation (6) in addition to the numerical results. A value of $\beta = 1.25$ has been used, which is in the range of the numerical simulations and in agreement with field tests (Peuchen et al., 2010). Overall, numerical results show a good agreement with the proposed interpretation technique.

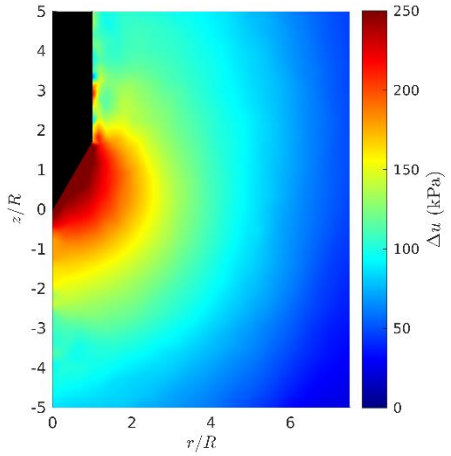

(a)

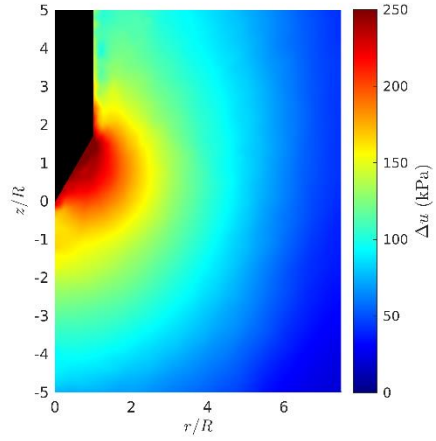

(b)

Figure 5. Comparison of the excess pore pressure for a rough soil-cone interface (a) and smooth interface (b). Material E. OCR = 1.6.

Given the assumption of undrained conditions in the analyses supporting the interpretation method, Equation (6) can only be used when CPTu is indeed undrained. However, undrained conditions might be difficult to identify as increasing the soil permeability has similar effects to decreasing the state parameter.

To highlight the differences on cone metrics of both effects, Figure 7 reports the numerical results presented in this work in addition to the numerical simulations of CPTu testing in partially drained and fully drained conditions presented in Monforte et al. (2021, 2023a), that assumed similar constitutive parameters. In the chart proposed by Robertson (1991), it is not possible to distinguish between changes in drainage conditions or the state parameter; decreasing the state parameter has exactly the same effect than increasing the permeability: the normalized cone resistance increases whereas the excess pore pressure decreases. However, in the Schneider et al. (2008) chart, both effects can be clearly differentiated: both $B_q Q_t$ and Q_t increase as the state parameter increases; instead, Q_t increases and $B_q Q_t$ decreases when larger permeabilities are considered.

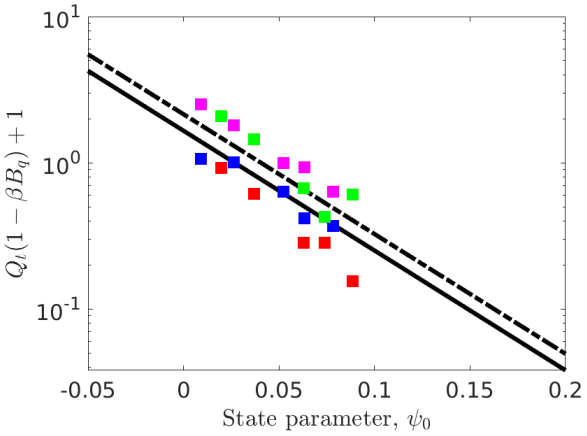

(a)

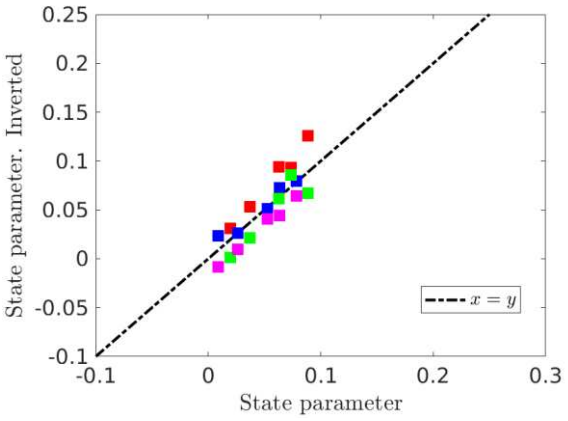

(b)

Figure 6. State parameter in terms of the modified normalized effective tip resistance, (a). Comparison of the input state parameter and that deduced by the interpretation technique, (b).

5 CONCLUSIONS

The derivation of the state parameter from CPTu readings is not a task exempt of uncertainty, partly because current interpretation techniques are still based on the solution of simplified problems (i.e., cavity expansion). With the advance of computational modelling, it is now possible to simulate cone testing with the actual geometry and with constitutive models capable of describing the response of liquefiable materials. Given the encouraging results obtained, it is likely that further advance

in the interpretation of CPTu results will be supported by advanced numerical modelling, such as that presented in this work.

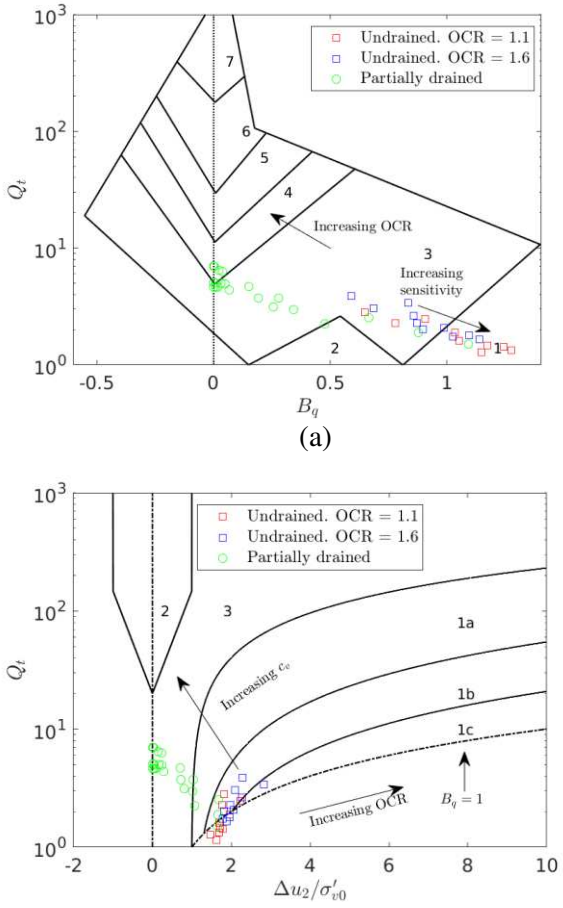

Figure 7. Numerical simulations of CPTu in interpretation charts: Robertson (1991), (a), and Schneider et al. (2008), (b).

6 ACKNOWLEDGEMENTS

Authors acknowledges financial support of Ministerio de Ciencia e Innovación of Spain (MCIN/AEI/10.13039/501100011033) through the Severo Ochoa Centre of Excellence project (CEX2018-000797-S) and research project PID2020-119598RB-I00.

7 REFERENCES

Arroyo, M., Gens, A. 2021. Computational analyses of Dam I failure at the Corrego de Feijao mine in Brumadinho. Final Report; available at https://www.mpf.mp.br/mg/sala-de-imprensa/docs/2021/relatorio-final-cinme-upc-1

Carbonell, J. M., Monforte, L., Ciantia, M.O., Arroyo, M., Gens, A. (2022). Geotechnical particle finite element method for modeling of soil-structure interaction under large deformation conditions. *Journal of Rock Mechanics and Geotechnical Engineering*, **14**(3), 967-983.

Fourie, A.B., Blight, G.E. Papageorgiou, G. 2001. Static liquefaction as a possible explanation for the Merriespruit dam failure. *Canadian Geotechnical Journal*, **38**, 707-719.

Jefferies, M, Been, K. 2016. *Soil liquefaction: a critical state approach*. 2nd edition. Taylor & Francis.

Mahmoudi, Y., Cherif Taiba, A., Hazout, L., Belkhatir, M., Baille, W. 2020. Packing density and overconsolidation ratio effects on the mechanical response of granular soils. *Geotechnical and Geological Engineering*, **38**(1), 723-742.

Mánica, M.A., Arroyo, M., Gens, A., Monforte, L. 2022 Application of a critical state model to the Merriespruit tailings dam failure. *Proceedings of the Institution of Civil Engineers – Geotechnical Engineering*, **175**(2), 151-165.

Mo, P.Q., Yu, H.S. 2017. Undrained cavity expansion analysis with a unified state parameter model for clay and sand. *Géotechnique*, **67**(6), 503-515.

Monforte, L., Arroyo, M., Carbonell, J.M., Gens, A. 2018. Coupled effective stress analysis of insertion problems in geotechnics with the particle finite element method. *Computers and Geotechnics*, **101**, 114-129.

Monforte, L., Gens, A., Arroyo, M., Mánica, M., Carbonell, J.M. 2021. Analysis of cone penetration test in brittle liquefiable materials. *Computers and Geotechnics*, *134*:104123.

Monforte, L., Carbonell, J.M., Arroyo, M., Gens, A. 2017. Performance of mixed formulations for the particle finite element method in soil mechanics problems. *Computational Particle Mechanics*, **4**(3), 269-284.

Monforte, L., Arroyo, M., Gens, A. 2023a. A relation between undrained CPTu results and the state parameter for liquefiable soils. *Canadian Geotechnical Journal* https://doi.org/10.1139/cgj-2022-0377

Monforte, L., Collico, S., Arroyo, M., Gens, A. 2023b. State parameter from CPTu: a comparison of interpretation techniques. *Under review.*

Oñate, E., Idelsohn, S.R., del Pin, F., Aubry, R. 2004. The particle finite element method-an overview. *International Journal of Computational Methods*, **1**(2), 267-307.

Pezehski, A., Ahmadi, M.M. 2022. In situ state of tailing silts using a numerical model of piezocone penetration test developed by Norsand model. *International Journal of Geomechanics,* **22**(1), 04021264.

Plewes, H.D., Davies, M.P., Jefferies, M.G. 1992. CPT based screening procedure for evaluating liquefaction susceptibility. *In Proceedings of the 45th Canadian geotechnical Conference*, Toronto, Canada.

Peuchen, J., Vanden Berghe, J.F., Coulais, C. 2010. Estimation of the u1/u2 conversion factor for piezocone. In *CPT'10, 2nd International Symposium on Cone Penetration Testing*.

Robertson, P.K. 1991. Soil classification using the cone penetration test: Reply. *Canadian Geotechnical Journal*, **29**(1), 46-57.

Schneider, J.A., Randolph, M.F., Mayne, P.W., Ramsey, N.R. 2008. Analysis of factors influencing soil classification using normalized piezocone tip resistance and pore pressure parameters. *Journal of Geotechnical and Geoenvironmental Engineering*, **134**(11), 1569-1586.

Yu, H.S. 1998. CASM: A unified state parameter model for clay and sand. *International Journal for Numerical and Analytical Methods in Geomechanics,* **22**, 621–653.